A Novel Framework for Integrating Data Mining with Control Loop Performance Assessment

Laya Das
Dept. of Electrical Engineering, Indian Institute of Technology Gandhinagar, Ahmedabad 382424, Gujarat India

Babji Srinivasan
Dept. of Chemical Engineering, Indian Institute of Technology Gandhinagar, Ahmedabad 382424, Gujarat India

Raghunathan Rengaswamy
Dept. of Chemical Engineering, Indian Institute of Technology Madras, Chennai 600036, Tamil Nadu India

DOI 10.1002/aic.15042
Published online September 30, 2015 in Wiley Online Library (wileyonlinelibrary.com)

Data driven control loop performance assessment techniques assume that the data being analyzed correspond to single plant-controller configuration. However, in an industrial setting where processes are affected due to the presence of feedstock variability and drifts, the plant-controller configuration changes with time. Also, user-defined benchmarking of control loops (common in industrial plants) requires that the data corresponding to optimal operation of the controller be known. However, such information might not be available beforehand in which case it is necessary to extract the same from routine plant operating data. A technique that addresses these fundamental requirements for ensuring reliable performance assessment is proposed. The proposed technique performs a recursive binary segmentation of the data and makes use of the fact that changes in controller settings translate to variations in plant output for identifying regions corresponding to single plant-controller configurations. The statistical properties of the data in each such window are then compared with the theoretically expected behavior to extract the data corresponding to optimal configuration. This approach has been applied on: (1) raw plant output, (2) Hurst exponent, and (3) minimum variance index of the process data. Simulation examples demonstrate the applicability of proposed approach in industrial settings. A comparison of the three routes is provided with regard to the amount of data needed and the efficacy achieved. Key results are emphasized and a framework for applying this technique is described. This tool is of significance to industries interested in an automated analysis of large scale control loop data for multiple process variables that is otherwise left unutilized. © 2015 American Institute of Chemical Engineers *AIChE J*, 62: 146–165, 2016

Keywords: control loop performance assessment, minimum variance index, Hurst exponent, interval halving, nonstationary data analysis

Introduction

One of the key factors determining the productivity of a plant is the performance of control loops. Maintaining controller performance at the desired level is, therefore, of prime importance to any industry. Often, a large percentage (up to 60%) of the control loops is found to underperform.[1] Routine performance assessment of these loops is, therefore, crucial for assessing plant-wide efficiency and quality[2] of industries. Techniques to assess control loop performance from plant output data have been studied extensively in the literature. The framework of minimum variance control (MVC) has been studied and applied widely for control loop performance assessment (CLPA) of linear and nonlinear, single input single output (SISO)[3–5] as well as multiple input multiple output (MIMO) systems.[6–12] These techniques have also been validated on several industrial processes[2,13–17] and serve as excellent reviews of such techniques. A filter-based technique for obtaining the best achievable performance of MIMO systems has also been considered[18] which also demonstrates techniques for obtaining the optimal controller settings for alternate control configurations in multivariate systems using minimum variance index (MVI) as the metrics. The MVC-based techniques fit an appropriate time series model such as autoregressive moving average (ARMA) to the plant output and estimate the theoretical minimum variance that is achievable using the minimum variance controller. The actual variance of plant output is then compared with this theoretical benchmark to assess the performance of control loop. A major requirement of the minimum variance-based performance assessment techniques is that the delay of the system be known beforehand, which is not always possible nor desirable to meet. This issue was addressed[19] using the Hurst exponent of plant

Correspondence concerning this article should be addressed to B. Srinivasan at babji.srinivasan@iitgn.ac.in.

output as an alternate measure of the control loop performance for SISO systems, which does not require prior knowledge of system delay. Performance assessment for set point tracking has also been addressed using the Hurst exponent.[20]

All the above CLPA techniques inherently assume that the data being analyzed corresponds to single plant-controller configuration and is stationary (in fitting a time series model or calculating the Hurst exponent). Moreover, in applying both the above approaches, such data were always assumed to be available. However, in an industrial setting where processes are affected due to the presence of feedstock variability and drifts, the statistical properties of plant output (and hence performance of control loop) vary with time. This implies that process data collected over time is nonstationary. For the CLPA measures to be meaningful, the data to be analyzed must then be carefully selected from plant measurements unless implemented online. Typically, in a plant with thousands of such interdependent control loops operating simultaneously, it is not possible to manually identify the correct data for performance assessment. Moreover, one of the key desired properties of any data driven performance assessment technique is that it be capable of automated background operation, including scheduled remote collection of control loop data and data integrity checks.[2] So, it is important to have a technique that can select the proper data for CLPA from a data historian and can be applied to numerous control loop variables simultaneously. Furthermore, user-defined benchmarking of control loops, which is not uncommon in the industry[8,17] requires that the optimal operating conditions (that have been practically achieved, as opposed to the theoretical optimum) of the controller be known. Extracting this information from the plant data is the first crucial step in such user-defined benchmarking. So, it is also desirable to be able to further locate segment(s) representative of optimal controller operation in a given data set.

In this work, we address the issue of optimally selecting such *appropriate* data segments from vast amounts of control loop data available from a process historian. We propose an interval halving technique for the former problem of data segmentation, followed by an analysis of the statistical properties of the data in each of these segments to identify the data corresponding to optimal operation. This article is organized as follows: we begin by providing the necessary background for characterizing performance of a control loop and motivate the need for addressing the above issues with a simulation example. The interval halving technique is then briefly introduced followed by a description of the proposed approach along with its two variants. Simulation results are presented for four benchmark systems and salient features of the technique are discussed along with the effect of certain tuning parameters followed by concluding remarks.

Background and Motivation

We begin by providing the background on MVI and scaling exponent methods for assessing the performance of control loops.

Measures of controller performance

In the MVC framework, the plant output is expressed as a stationary ARMA process[2]

$$\begin{aligned} y^{\mathrm{ref}}(t)-y(t)=\epsilon(t)&=\frac{B(q)}{A(q)}e(t)\\ y^{\mathrm{ref}}(t)-y(t)=\epsilon(t)&=(1+\psi_1 q^{-1}+\psi_2 q^{-2}+\ldots\\ &+\psi_{b-1}q^{-(b-1)}+\psi_b q^{-b}+\psi_{b+1}q^{-(b+1)}+\ldots)e(t) \end{aligned} \tag{1}$$

where $e(t)$ is an independent and identically distributed noise sequence, t denotes the sampling instants $t=kT$ (T is the sampling time), q is the time shift operator with $q^{-1}e(t)=e(t-1)$ and the coefficients ψ_i are obtained by long division of the polynomial $B(q)$ by $A(q)$. Here, $y(t)$ is the process output and $y^{\mathrm{ref}}(t)$ is the constant set point to the control loop with $\epsilon(t)$ representing the error data (deviations of the process output from set point). When MVC is achieved, $\epsilon(t)$ can be expressed as an MA process of order $b-1$, b being the process delay. This leads to the minimum achievable variance with any controller as $\sigma^2_{\mathrm{MV}}=\sigma_e^2\sum_{i=0}^{b-1}\psi_i^2$ with $\psi_0=1$. The MVI is then defined as the ratio of this minimum variance to the actual plant output variance. The MVC-based index therefore involves fitting a stationary ARMA model to $\epsilon(t)$ to estimate σ^2_{MV} and comparing this with the actual variance of $\epsilon(t)$. With improvement in controller performance, the variance of plant output decreases, with the minimum variance achieved under optimal controller configuration[3] in which case MVI reaches unity.

A critical requirement in estimating σ^2_{MV} is the knowledge of the parameter b, that is, the system delay. An alternative route that enables quantifying the performance of control loops while relaxing this requirement is to use the scaling exponent of the plant output error.[19] This measure originates from the MVC framework, but takes a different approach to assess the control loop performance. As indicated earlier, under optimal conditions, the error signal ($\epsilon(t)$) can be expressed as an MA($b-1$) process, with no correlation with itself after a lag of b time units. Under these conditions, the plant output has the least predictability. Predictability in plant output indicates a scope to model the process better and hence for improvement of controller performance.[19] Hence with deterioration of controller performance, the predictability of plant output increases. The scaling exponent, also called the Hurst exponent[21] quantifies this predictability and thereby the performance of control loop. Several methods have been proposed for estimating the scaling exponent of a time series[21–24] using both statistical as well as spectral properties of the time series. The detrended fluctuation analysis (DFA)[24] is a popular technique for estimating the Hurst exponent which has been used in earlier works[19] and in this work, whose computational details have been listed below.

1. The given time series y[k] is integrated after mean removal: $Y[k]=\sum_{i=1}^{k}(y[k]-\langle y\rangle)$.
2. The integrated series $Y[k]$ is divided into windows of length n and in each window, a least squares line $\hat{y}=ay+c$ is fit to the series.
3. The RMS fluctuation is then defined as

$$F(n)=\sqrt{\frac{1}{N}\sum_{i=1}^{N}(Y[i]-\hat{y}_i)^2}$$

   This is a function of the window size n with N denoting the total number of samples.
4. Steps 2 and 3 are repeated for varying window sizes n (ranging from 10 to $N/3$ for this work).

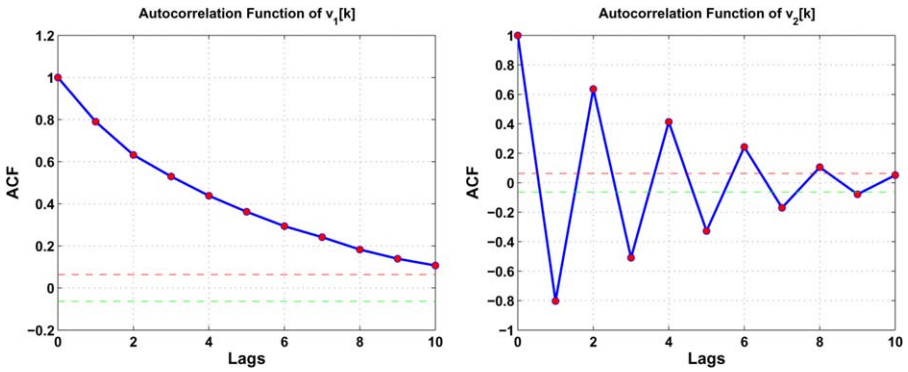

(a) (b)

Figure 1. Autocorrelation functions of two time series. (a) ACF indicates positive correlation ($\alpha = 0.6210$); (b) ACF indicates negative correlation ($\alpha = 0.3370$).

[Color figure can be viewed in the online issue, which is available at wileyonlinelibrary.com.]

5. A log–log plot of the fluctuation with window size is made, and the slope of this plot is calculated, which gives the desired estimate of α.

When a stationary time series is completely unpredictable with a linear model, the scaling exponent is equal to 0.5. A value lying between 0 and 0.5 indicates an antipersistent (negatively correlated) time series, while a value in the range 0.5–1.0 indicates persistence (positive correlation). Consider two time series generated from two different processes as

$$v_1[k] = 0.8v_1[k-1] + e[k]$$
$$v_2[k] = -0.8v_2[k-1] + e[k]$$

where $e[k]$ is a standard normal white noise sequence. The Hurst exponent calculated from DFA for the two series are 0.6210 and 0.3370, respectively. This indicates a positive correlation for the first series while a negative correlation for the second series which agree with the model definitions. The autocorrelation functions (ACFs) of the two series, plotted in Figure 1 also reflect similar behavior.

Under optimal conditions, the plant output being the least predictable, its scaling exponent is expected to be closest to 0.5. As the tuning deteriorates, the properties of error signal deviate from those of an MA($b-1$) process and the scaling exponent moves away from 0.5 (depending on the nature of correlation). This idea has been proposed for CLPA of SISO systems.[19]

In both the above approaches, the output error is assumed to be stationary. However, due to drifts and feedstock variability the process output data collected over time becomes nonstationary. So, before applying the CLPA techniques, it is necessary to identify stationary segments of data that correspond to single plant-controller settings and provide the segmented data to the assessment techniques. In summary, a unified approach toward CLPA should address the following issues:

1. Identification of data segments for performance assessment (data integrity)
2. Determination of the optimality of controller in the region of interest
3. Quantification of the scope for improvement that exists at any time
4. Be as automated as possible (to allow application of the tool routinely across thousands of loops)

We present three different routes that are aimed at addressing the above questions. As will be illustrated later, analyzing the variance of the error signal allows us to address only the first issue. However, the scaling exponent and MVI routes enable one to address all the above concerns simultaneously. We next list the contribution of this work and emphasize the significance of the proposed technique in a large-scale system, followed by a motivating example.

Significance and contribution

Although there is a vast repository of techniques for performance assessment of control loops, all of them assume availability of appropriate data to begin with. However, in a practical application with a large-scale system having thousands of control loops, selecting the appropriate data from large datasets is a time consuming task. In the absence of an automated data mining technique, all CLPA techniques are incomplete and not directly applicable to raw data. This problem has been identified for the first time in this article and a technique has been proposed to select the appropriate segments of data so that the existing techniques can be suitably applied. Integrating this novel approach with existing CLPA techniques will allow for a completely automated tool that can work with remote data.

Motivating example

We now present a motivating example for the need for addressing the problem of segmenting plant data into windows corresponding to single plant-controller configuration with an example. Consider a system described by (2) with the corresponding system matrices indicated in (3) and (4)

$$\begin{aligned} Y_t &= TU_t + Na_t \\ U_t &= -QY_t \end{aligned} \tag{2}$$

$$T = \frac{q^{-6}}{1-0.8q^{-1}} \tag{3}$$

$$N = \frac{1-0.2q^{-1}}{\nabla(1+0.4q^{-1})(1-0.3q^{-1})(1-0.5q^{-1})} \tag{4}$$

$$\begin{aligned} Q &= K_p + \frac{K_i}{1-q^{-1}} \\ &= \frac{(K_p+K_i)-K_pq^{-1}}{1-q^{-1}} \end{aligned} \tag{5}$$

A Proportional integral (PI) controller of the form (5) is implemented on the plant. Seven different controller settings

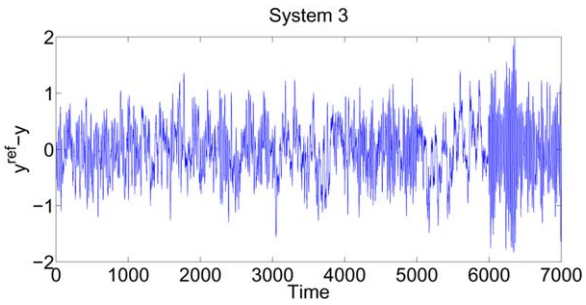

Figure 2. Sample output of a plant with seven different controller configurations.

[Color figure can be viewed in the online issue, which is available at wileyonlinelibrary.com.]

have been simulated for the system. The notation followed in Ref. 25, that is, $Q=\frac{a+bq^{-1}}{\nabla}$ has been used here where ∇ is the shorthand notation for $1-q^{-1}$. The outputs have been concatenated and plotted in Figure 2 with settings listed in Table 1.

From a visual inspection, it is clear that one cannot identify the regions corresponding to fixed settings, and further the optimal region in the data. However, the data from time indices 1 to 1000, 1001 to 2000, and so on correspond to different fixed controller settings.

Tables 2 and 3 demonstrate the effect of the amount of data chosen on the performance indices (MVI and scaling exponent of plant output). It is clear that the amount of data selected for performance assessment affects the indices calculated, because the statistical properties of the data are varying over time although they are not visually obvious. If CLPA technique is presented with data from combination of different regions (as shown in Tables 2 and 3), the measure obtained could lead to the following: (1) Type I error, where there is real possibility of performance improvement while it is not indicated by the CLPA tool, or (2) Type II error in which CLPA indicates a possible improvement although the control loop is optimal. Moreover, notice that the deviation of the indices from the correct values does not follow any particular pattern—in some cases, the performance is underestimated, while in others it is overestimated. This rules out a heuristic approach for making calculated guess of the actual performance indices, clearly demonstrating that for the performance indices to be meaningful, there is a need to automatically identify the appropriate segment(s) of data.

Now, consider a situation in which CLPA has been performed with properly selected data, and one has a series of indices (MVI or scaling exponent) generated as discussed in Remark 1. Such a situation is depicted in Figure 3 for a multivariate system taken from Ref. 26 in which the scaling exponents for 11 different configurations (for one of the outputs) are concatenated. From the data, it is difficult to identify the number of segments and the location of such segments. So, to use such data to perform user-defined benchmarking, it is necessary to identify the 11 segments, quantify the scope for improvement in each such segment and identify the segment corresponding to optimal operation. With thousands of control loops in an industry, this is a tedious but an important task.

Table 1. List of Controller Parameters for Motivation Example

Data Index	a	b
1–1000	0.21180	−0.18960
1001–2000	0.16944	−0.15168
2001–3000	0.25416	−0.22752
3001–4000	0.12708	−0.11376
4001–5000	0.29652	−0.26544
5001–6000	0.08472	−0.07584
6001–7000	0.33888	−0.30336

Table 2. Effect of the Data Selected on the Performance Indices

Data Index	MVI
1–1000	0.64398
1–1800	0.65968
1–3000	0.64211
1–7000	0.54692
2001–3000	0.54375
2001–3500	0.57140
2001–4500	0.60269
2001–7000	0.49985

Both the above problems emphasize the need for a technique to perform data segmentation and subsequent identification of optimum window. To perform data segmentation to identify stationary data segments, interval halving approach is one of the suitable methods that is used in this work and is described next.

Interval halving

The problem of breaking a given nonstationary signal into segments of stationary signal can be considered as one of change-point detection, which has been extensively studied.[27–30] Both time and frequency domain techniques exist for detecting multiple change points in a time series. Such techniques have been applied to fields as diverse as econometrics for detecting structural breaks in financial data and process control for detecting changes in process behavior. Interval halving is a time domain binary segmentation-based search algorithm used to locate regions of interest in a signal. In this article, this technique has been used to detect and locate changes in the structure (statistical properties) of signal. Interval halving works recursively by splitting a given signal into two halves at every iteration and eliminating that half which does not satisfy certain criteria. This technique has been used for automated identification and qualitative analysis of process trends[31,32] and for fault diagnosis.[33,34]

In this work, an interval halving-based change point detection algorithm that closely follows the method outlined in Ref. 31 is proposed for data segmentation. The algorithm begins by splitting the data into two halves and checking for stationarity in each half based on statistical tests. A window identified as

Table 3. Effect of the Data Selected on the Performance Indices

Data Index	α
1–1000	0.68776
1–1800	0.62152
1–3000	0.63134
1–7000	0.65989
2001–3000	0.81491
2001–3500	0.88773
2001–4500	0.85363
2001–7000	0.71701

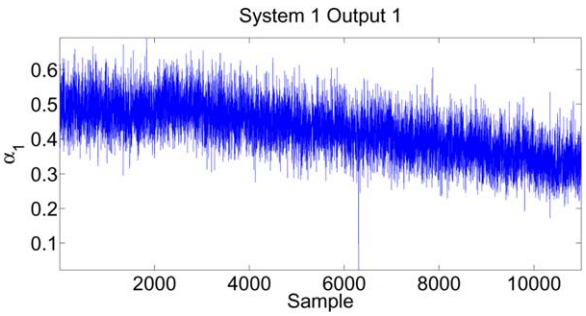

Figure 3. Sample scaling exponent data of a plant with 11 different controller configurations (data generated as discussed in Remark 1).

[Color figure can be viewed in the online issue, which is available at wileyonlinelibrary.com.]

stationary is saved and the next window is processed. However, if the test indicates nonstationarity, interval halving is performed again till the data in each window is stationary or a minimum window size is reached. Details of this algorithm are presented in Flowchart 1. There are, however, situations where this algorithm can fail in detecting nonstationary. This can happen, for example, when there are oscillatory behaviors at large time scales. A test for the goodness of fit needs to be performed for every window to handle such situations—a poor goodness of fit would call for a forceful interval halving. These details are provided in subsequent sections. The versatility of this technique lies in the fact that the decision for interval halving is based on statistical tests for certain parameters. This allows for detection of different types of nonstationarity using the same algorithm using appropriate statistical tests.

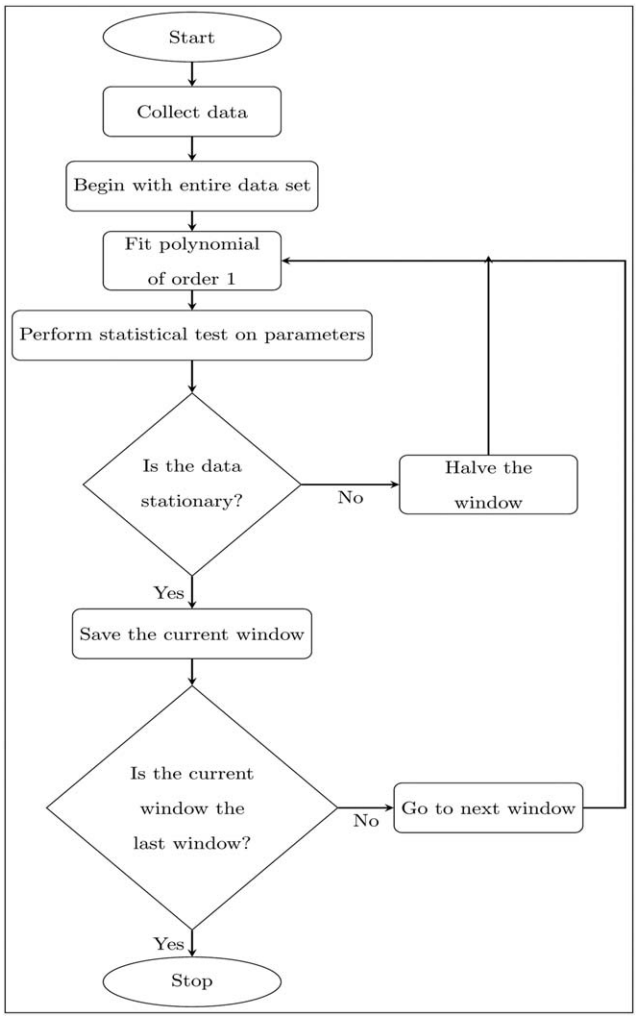

Flowchart 1. Plain Interval halving algorithm.

Proposed Methodology

In this section, the proposed approach to address the problems of data segmentation, optimal dataset selection, and performance assessment in all segments is presented. We begin by describing the type of nonstationarity encountered with the data followed by the assumptions made about the process and develop techniques to address each one of them.

Types of nonstationarity

The plant output error (ϵ), for a single plant-controller configuration will have a constant variance. When the plant or controller settings change, the variance of plant output error will increase or decrease depending on the optimality of the setting. So, when provided with ϵ data, one encounters variance nonstationarity.

Conversely, the scaling exponents calculated for a single plant-controller configuration will have a constant mean with a finite variance. When the configuration changes, there is a shift in the average value of scaling exponents. The same effect will be observed with the MVI data over time. So, the performance indices evaluated over time will exhibit mean nonstationarity.

Assumptions

The techniques for addressing the nonstationarity in data are developed under the following assumptions:

1. The plant and controller structures are assumed to be of the transfer function and PI controller type, described by Eqs. 8 and 5, respectively. The controller structure being a PI controller, the framework does not account for any constraints in the system.
2. The variation in plant-controller settings are assumed to be at a rate which will allow the interval halving method (through an automatic iterative procedure, discussed later) to identify stationary segments of data. A brief discussion on the choice of windows (used by the interval halving algorithm) to detect these segments is provided later.
3. The interval having algorithm (described later) basically looks for segments which are invariant as far as the properties of interest are concerned. As a result, if there are variations in the delay within the larger data, then those will be automatically identified as being in different regions, provided they result in either mean or variance nonstationarity. However, if the discrimination between segments is made using MVI, then within the smaller segments, one has to assume that the time delay is constant and this might lead to inaccuracies. As a result, if changes in time delay are suspected in any real life system then it would be advisable to use scaling exponent route for CLPA.

Variant 1: Addressing variance nonstationarity with interval halving

The key feature of ϵ data in the presence of multiple configurations is variance nonstationarity. The proposed technique involves an interval halving procedure, which involves recursively detecting the presence of such nonstationarity, and dividing the data into two segments. To detect the presence of a time dependence of the variance of the signal, a statistical test for presence of heteroskedasticity has been used in this work, which is then integrated with the data segmentation procedure.

The general heteroskedasticity test[35] is used to determine whether the estimated variance of the residuals of a regression model is dependent on the independent variables (regressors). Consider a process as

$$y = ax + v$$

where y is the dependent variable, x is vector of k ($k \times 1$) independent variables (regressors), a is a vector ($1 \times k$) of parameters relating y to x and v is the noise corrupting the measurements of y. Let the model for the process be identified as $\hat{y} = \hat{a}x$ which yields residuals:

$$\hat{v} = y - \hat{y}$$

. To check for dependence of variance of residuals ($\sigma\hat{v}^2$) on the regressors x, the residuals are squared and regressed on to a set of test variables z as

$$\hat{v}^2 = \beta z \tag{6}$$

where the coefficients β are functionally unrelated to a. The test variables can be[35] the regressors or the squared regressors as in the commonly used Breusch Pagan test.[36] Then, to check for the heteroskedasticity of residuals with respect to the regressors the following test statistic can be used[35]

$$T = R^2 N$$

with R^2 being the coefficient of determination of the regression of the squared residuals on the test variables, (6) and N being the sample size. The coefficient of determination R^2 can be obtained as

$$R^2 = 1 - \frac{\sum_i (y_i - \hat{y}_i)^2}{\sum_i (y_i - \bar{y})^2}$$

where $\bar{y}$ is the sample mean of y. The test statistic T follows a χ^2 distribution with $p - 1$ (with p being the number of coefficients, β) degrees of freedom.

In our application, we are interested in detecting the dependence of variance of $\epsilon(t)$ on time. So, by squaring the plant output error and regressing on time as

$$\epsilon^2 = \beta_0 + \beta_1 t \tag{7}$$

we can detect the functional dependence of σ_ϵ^2 on time, and hence variance nonstationarity of ϵ. From (7), it is clear that $p = 2$ which leads to a χ_1^2 distribution for the T statistic of the test. This resulting statistic can be used to check for a functional dependence of the variance on time. This test has to be performed at every iteration to test for heteroskedasticity, and based on the results of this test, a decision on splitting of the data has to be taken. This heteroskedasticity test coupled with interval halving is depicted in Flowchart 2.

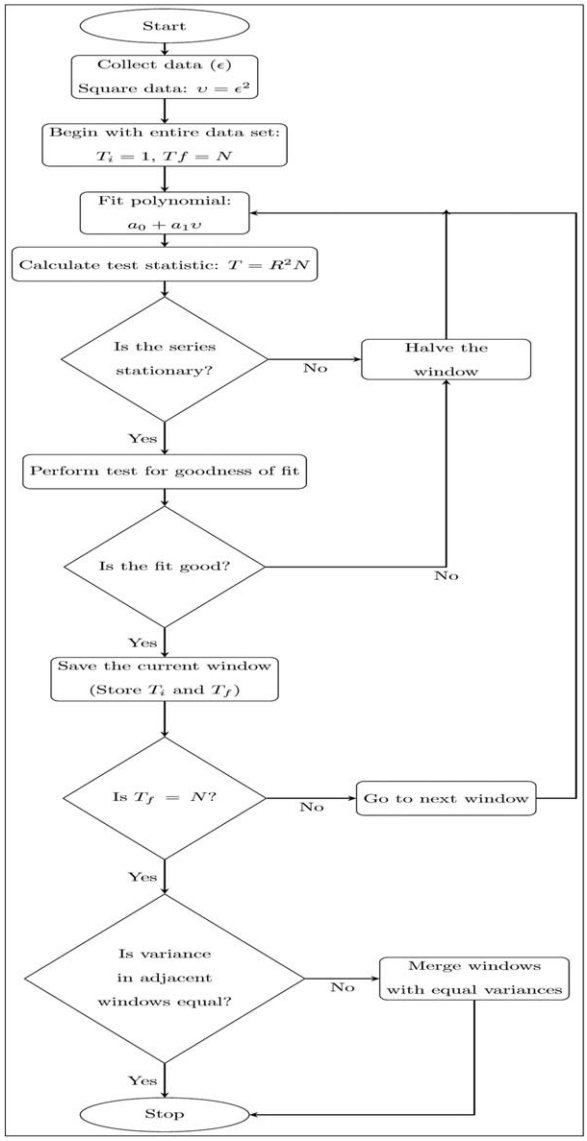

Flowchart 2. Test for heteroskedasticity coupled with interval halving algorithm to address variance nonstationary (ϵ) data.

This also includes the additional tests for goodness of fit needed to ensure proper data segmentation and a test for equality of variance in two adjacent windows to ensure that one does not have more windows than necessary to explain the data.

Variant 2: Addressing mean nonstationarity with interval halving

The scaling exponent and MVI calculated for a single plant-controller configuration will have a constant mean with a finite variance but a statistically insignificant slope. However, when the configuration changes there is a shift in the average value of the indices. For instance, when the configuration is fixed, the average value of scaling exponents will be fixed at α_1, while in the presence of two different configurations, the average will change from α_1 to α_2 over time. This will result in a finite nonzero slope for the dataset. So, by fitting a linear polynomial to the data at every iteration and checking the

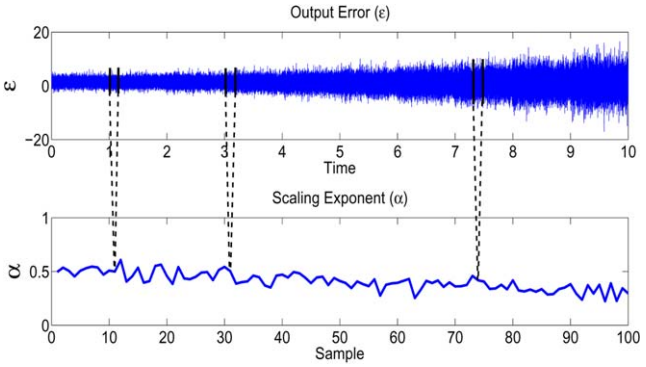

Figure 4. Comparison of amount of data required for the two variants.

In both the plots, 10 different plant-controller configurations are present. While only 1000 data points for ϵ data are required for each configuration (upper plot) resulting in a total of 100,000 data points, this scales up to 1000 × 1000 data points for α (or MVI) data (lower plot) leading to only 100 data points for the same ϵ data. This is because every 1000 ϵ data points scale down to one α value, as shown in the figure for three representative cases. [Color figure can be viewed in the online issue, which is available at wileyonlinelibrary.com.]

statistical significance of parameters, mean stationarity of the data can be examined.

The interval halving technique applied to the scaling exponent or MVI data works as follows:

1. A first-order polynomial of the form: $x(t)=a_0+a_1t$ is fit to the data, where $x(t)$ can be the scaling exponent or MVI data.
2. The statistical significance of a_1 is checked. If a_1 is not significant, then the data is stationary and hence corresponds to a single plant-controller setting. If however, a_1 is significant then there is a time dependence of the mean of the data and hence it is nonstationary. The data are now broken into two windows of equal length and the above step is repeated till a window is reached in which the slope of the polynomial is statistically insignificant. The data in this window then corresponds to a single plant-controller tuning.
3. The above procedure is repeated till the entire data have been processed.

Similar to Variant 1, equality of mean in two adjacent windows is checked. If they are found to be statistically equal, then the windows are joined together to ensure that one does not have more windows than necessary to explain the data. The interval halving for handling mean nonstationarity is depicted in Flowchart 3.

In both the above variants, interval halving is performed only up to a certain minimum window size, below which the data are not split any further. This ensures that the algorithm stops after a finite number of iterations. The interval halving algorithm along with associated statistical tests identifies segments of stationary data that correspond to single plant-controller configurations. The next objective is to determine the segment(s) representative of optimal operation of the loop (such information is desired for user-defined benchmarking of control loops). The segment corresponding to optimal configuration can be identified as the one with

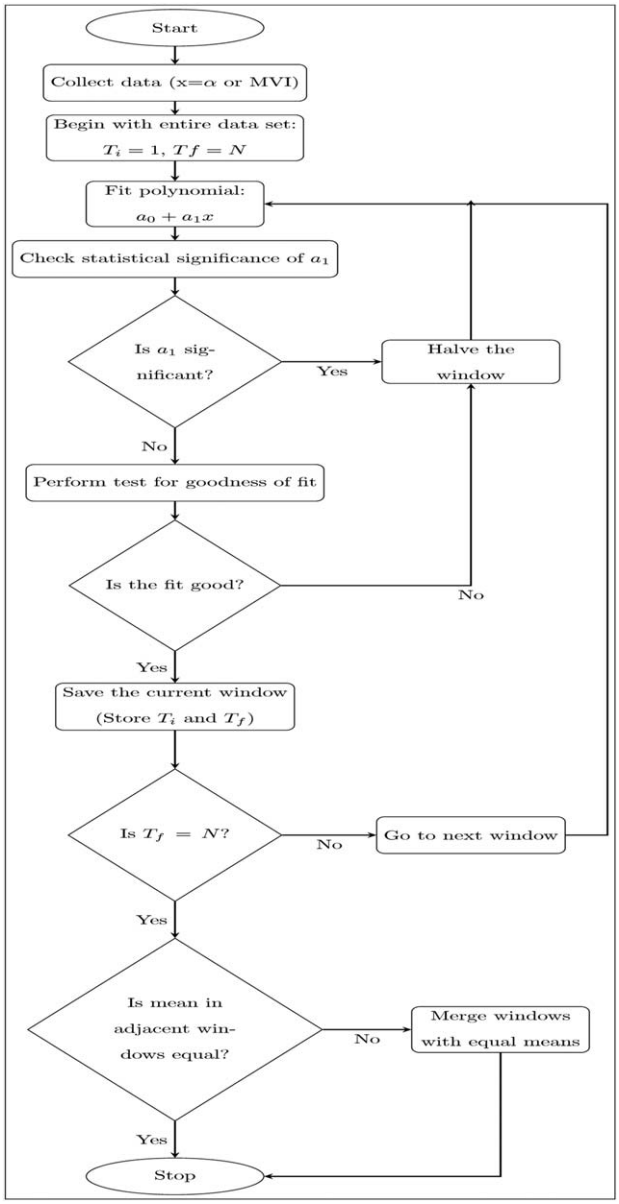

Flowchart 3. Interval halving algorithm to address mean nonstationary (α or MVI data).

the least variance for ϵ data, the minimum absolute distance from 0.5 for α data or the minimum distance from 1 for MVI data.

Remark 1. *Note that scaling exponent and MVI are performance measures in themselves and require that the data they process belong to a fixed configuration. In a practical situation, this can be performed without the knowledge of the fixed or varying controller configurations by having a moving window for calculating the scaling exponent or MVI of plant output. Whenever there is a change in the configuration the scaling exponents and MVI's will start deviating from their previous value and settle around a different average value, indicating a change in the configuration. However, this imposes a bound on the lowest feature size that can be detected by the interval halving algorithm. For instance, if one is interested in detecting a stationary window of size n, then with the ϵ data, n samples are sufficient to detect the same.*

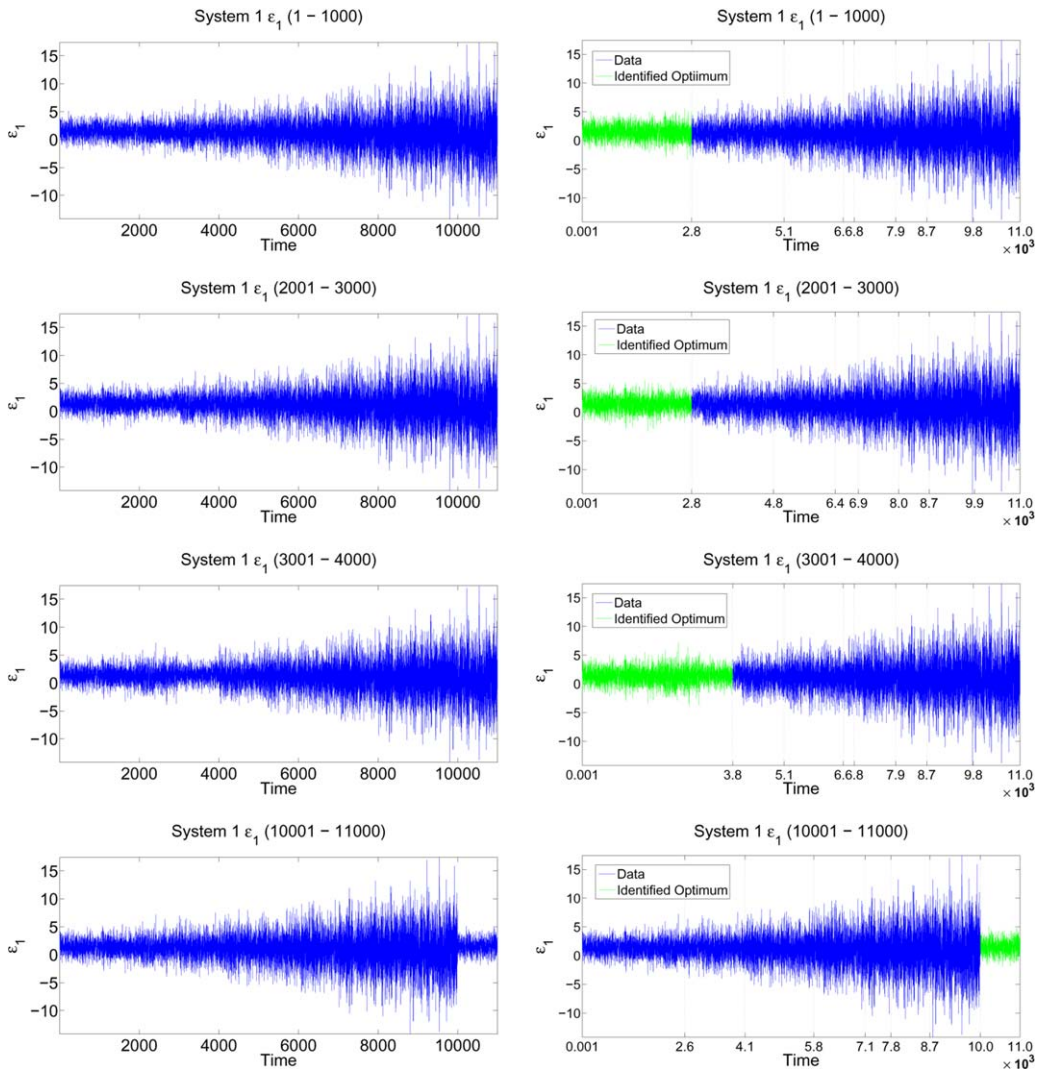

Figure 5. Identification of data segment corresponding to optimal configuration for System 1 using error data ($\epsilon_1(t)$).

Left column plots show the raw data and right column plots show the data after segmentation and identification. Green portion represents the identified optimal settings while the true optimal settings for each case are specified in the title of each plot. For example, in the last plot, true optimum lies in 10,001–11,000 and identified optimum is 10,000–11,000. [Color figure can be viewed in the online issue, which is available at wileyonlinelibrary.com.]

However, with the latter routes, one needs to have $1000\times n$ *contiguous samples of* ϵ *belonging to a single plant-controller configuration from which n samples of* α *or MVI can be calculated (assuming one sample of* α *or MVI is calculated from 1000 samples of* ϵ*). So, using* ϵ *route needs less data and hence a coarser sampling can be allowed. Conversely, to use the latter routes, a finer sampling is necessary. This might seem like a restrictive requirement, but with advances in Distributed Control System (DCS) which allow large sampling rates, such amounts of data can be made available. This is illustrated in Figure* 4 *in which the upper figure is a plot of the output error and the lower figure is a plot of the scaling exponent. Every point on the plot of scaling exponent is derived from 1000 points on the output error plot. So, the scaling exponent as well as MVI data actually involve an appropriately scaled amount of data.*

Remark 2. *When the error data* $\epsilon(t)$ *is used, one can only identify segments corresponding to single plant-controller settings and their variances. Although the segment of data having the least variance can be considered as the best of all the configurations available in the data, it is not necessarily the theoretically optimal configuration and does not provide a quantitative information about the extent by which performance can be improved. This is unlike the scaling exponent (or MVI) route where a value closest to 0.5 (or 1) indicates optimal operation of the control loop. This is a distinct advantage of using scaling exponent or MVI routes for data mining.*

Simulation Results

We now demonstrate the proposed approach on different benchmark systems taken from Refs. 25 and 26. Both univariate and multivariate systems have been considered. However, in the multivariate systems, only one output is considered and the identification procedure is performed.

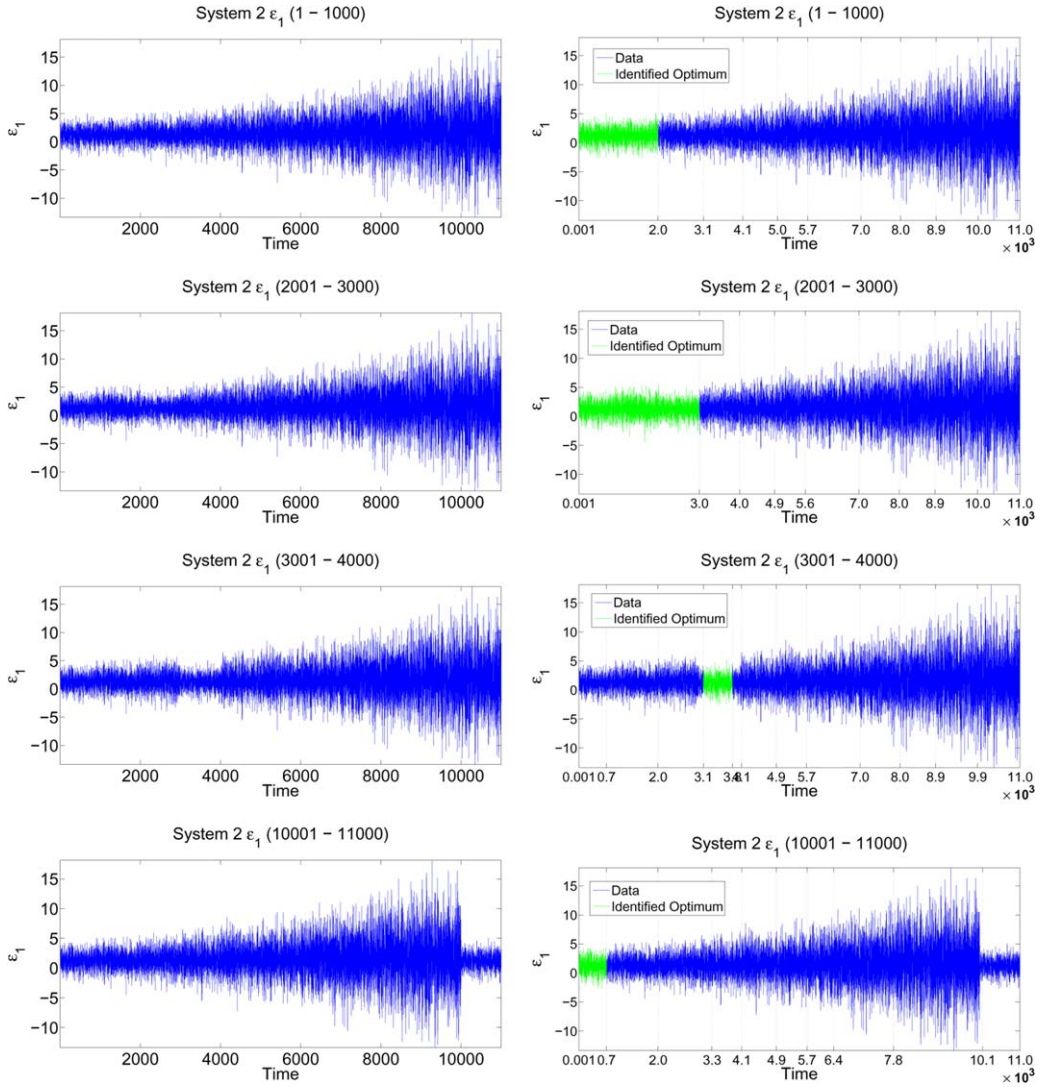

Figure 6. Identification of data segment corresponding to optimal configuration for System 2 using error data ($\epsilon_1(t)$).

Left column plots show the raw data and right column plots show the data after segmentation and identification. Green portion represents the identified optimal settings while the true optimal settings for each case are specified in the title of each plot. For example, in the third plot, true optimum lies in 3001–4000 and identified optimum is 3100–3800. [Color figure can be viewed in the online issue, which is available at wileyonlinelibrary.com.]

System description

All the systems considered in this work can be described as

$$\begin{aligned} Y_t &= TU_t + Na_t \\ U_t &= -QY_t \end{aligned} \tag{8}$$

where U_t and Y_t are the input and output of the plant, respectively, and a_t is the external disturbance (white noise). T and N describe the dependence of output on the input and noise, respectively, and Q describes the controller operation. For univariate systems, T, N, and Q are single functions of the time shift operator q^{-1}, whereas for multivariate systems they are matrices of appropriate dimensions. Two univariate and two multivariate systems have been considered in this work, which are described below.

The first two systems are multivariate systems taken from Ref. 26. System 1 is described using the following transfer function matrices

$$T = \begin{bmatrix} \dfrac{q^{-1}}{1-0.4q^{-1}} & \dfrac{K_{12}q^{-2}}{1-0.1q^{-1}} \\ \dfrac{0.3q^{-1}}{1-0.1q^{-1}} & \dfrac{q^{-2}}{1-0.8q^{-1}} \end{bmatrix}$$

$$N = \begin{bmatrix} \dfrac{1}{1-0.5q^{-1}} & \dfrac{-0.6}{1-0.5q^{-1}} \\ \dfrac{0.5}{1-0.5q^{-1}} & \dfrac{1}{1-0.5q^{-1}} \end{bmatrix}$$

$$Q = \begin{bmatrix} \dfrac{0.5-0.2q^{-1}}{1-0.5q^{-1}} & 0 \\ 0 & \dfrac{0.25-0.2q^{-1}}{(1-0.5q^{-1})(1+0.5q^{-1})} \end{bmatrix}$$

System 2 is described by the following matrices

$$T=\begin{bmatrix} \frac{q^{-1}}{1-0.4q^{-1}} & \frac{K_{12}q^{-2}}{1-0.1q^{-1}} & \frac{0.2q^{-2}}{1-0.5q^{-1}} \\ \frac{0.7q^{-1}}{1-0.2q^{-1}} & \frac{q^{-2}}{1-0.8q^{-1}} & \frac{0.8q^{-2}}{1-0.7q^{-1}} \end{bmatrix}$$

$$Q=\begin{bmatrix} \frac{0.5-0.2q^{-1}}{1-0.5q^{-1}} & 0 \\ 0 & \frac{0.25-0.2q^{-1}}{(1-0.5q^{-1})(1+0.5q^{-1})} \\ \frac{0.6-.01q^{-1}}{1-q^{-1}} & \frac{0.6-.01q^{-1}}{1-q^{-1}} \end{bmatrix}$$

The noise matrix N for this system is the same as that of System 1. For the above two systems, the parameter K_{12} of transfer function matrix T is varied from 0 to 10 in steps of 1, as has been done in Ref. 26 with the best performance obtained with $K_{12}=0$. Both the multivariate systems considered here have two outputs. However, in both the cases only one of the outputs is observed to be sensitive to controller tuning and the same has been considered for identification of optimal operating conditions.

The next two systems are univariate systems taken from Ref. 25. System 3 is described as follows ($\nabla=1-q^{-1}$)

$$T=\frac{q^{-6}}{1-0.8q^{-1}}$$

$$N=\frac{1-0.2q^{-1}}{\nabla(1+0.4q^{-1})(1-0.3q^{-1})(1-0.5q^{-1})}$$

while the last system (System 4) is described as follows

$$T=\frac{q^{-6}}{1-0.8q^{-1}} \tag{9}$$

$$N=\frac{1+0.6q^{-1}}{\nabla(1-0.5q^{-1})(1-0.6q^{-1})(1+0.7q^{-1})} \tag{10}$$

For both the systems, a PI controller of the form

$$\begin{aligned} Q&=K_p+\frac{K_i}{1-q^{-1}} \\ &=\frac{(K_p+K_i)-K_pq^{-1}}{\nabla} \end{aligned} \tag{11}$$

is implemented. The parameters K_i and K_p are the tuning parameters for the above systems whose optimal values are provided in Ref. 25.

Procedure

In each of the above cases, simulations proceeded in the following manner: the system (plant and controller) configuration is fixed and it is simulated for a certain fixed amount of time (e.g., 1000 data points); the parameters are then varied from their optimal values to affect the controller performance and a number of such configurations are considered. The use of scaling exponent or MVI for assessing the performance, however, requires much more data than using the error data directly. This is because the scaling exponent or MVI is calculated for a large number of data points (in our case, 1000 data points). Moreover, the use of MVI requires the knowledge of system delay. As a result, to get say 100 values of α corresponding to a single plant-controller configuration, one would require 100 $\times$ 1000 data points of ϵ. This is performed by simulating the system for a number of times (100) for a fixed configuration, by varying the noise sequences. However, one can also have a moving window for calculation of the scaling exponent or MVI, which reduces the number of data points required.

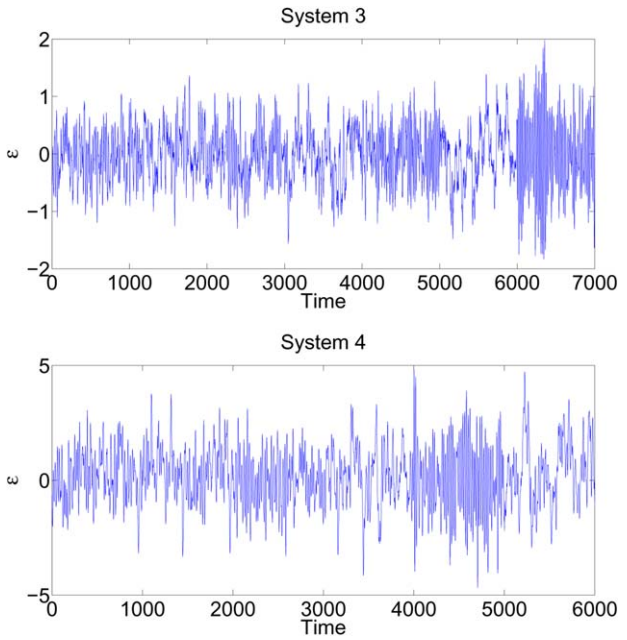

Figure 7. Sample output errors of Systems 3 and 4 with different controller configurations.

Note that for both the systems the change in variance is not significant to be detected. So, the proposed technique cannot be applied reliably on this data. [Color figure can be viewed in the online issue, which is available at wileyonlinelibrary.com.]

Realizations corresponding to different system configurations are ordered in various ways to generate different combinations of controller or plant parameter evolution. This nonstationary signal is then analyzed for identifying the window corresponding to the optimal configuration. Finally, the window identified as the optimal one is compared with the true optimal window to assess the reliability of the proposed technique.

We now present the results of identification procedure with the proposed technique. In all the results presented here, there are two columns of plots in each figure. The left column contains plots of the data before the technique is applied. This is representative of the data that would be handed over to this tool. The second column contains plots indicating the location of the change points as detected by the tool and the window identified as the optimum one. The dashed lines represent time instants which are identified as change points in the data. The segment of the signal within two consecutive dashed lines is stationary. The segment of the signal that is identified as optimal is indicated in green, while the location of the true optimal window is indicated in the title of each figure. Only representative cases have been illustrated in the figures.

Simulation results: Variant 1 (variance of the error signal)

We first illustrate the results for the above systems using the variance of the error signal as the parameter of interest,

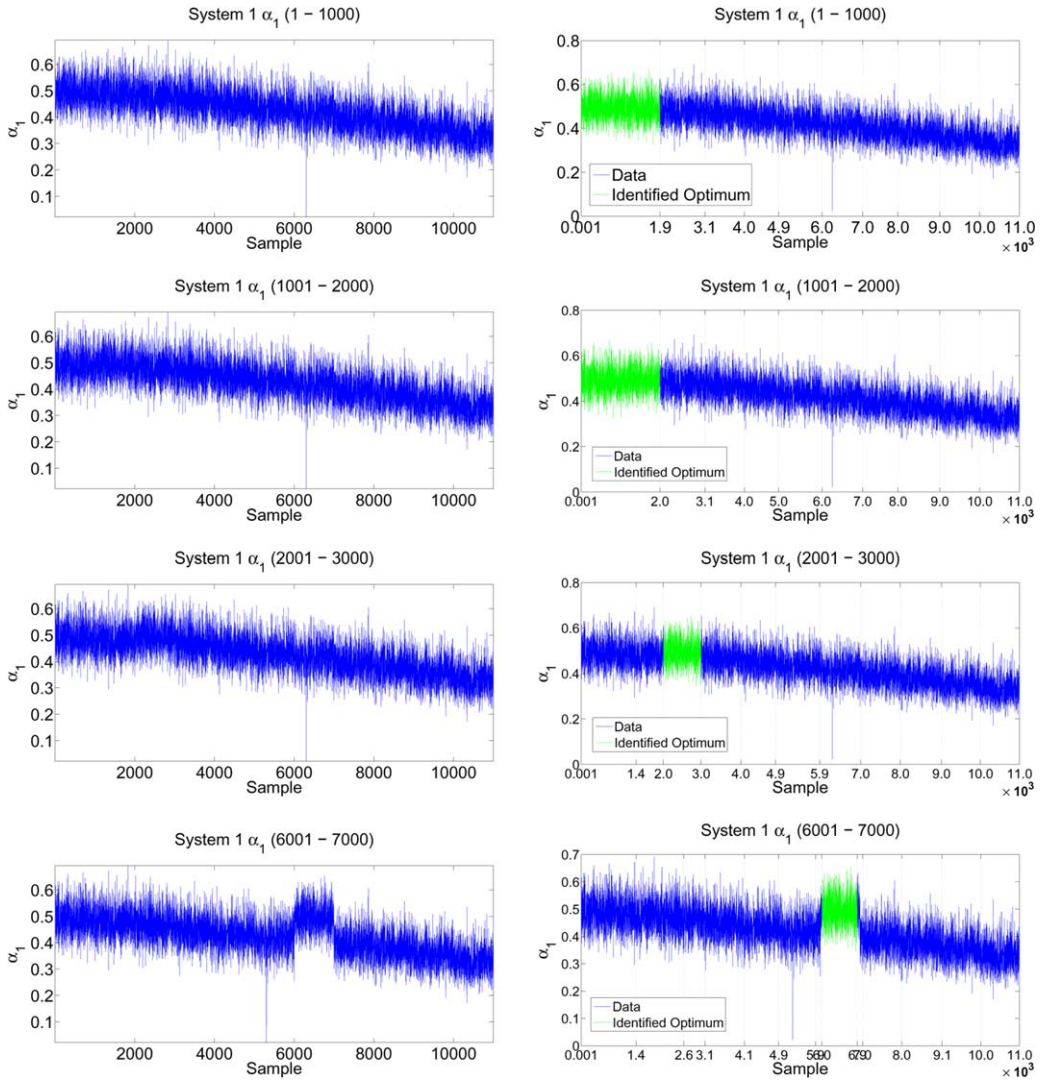

Figure 8. Identification of data segment corresponding to optimal configuration for System 1 using scaling exponent data ($\alpha_1(t)$).

Left column plots show the raw data and right column plots show the data after segmentation and identification. Green portion represents the identified optimal settings while the true optimal settings for each case are specified in the title of each plot. For example, in the last plot, true optimum lies in 6001–7000 and identified optimum is 6001–6900. [Color figure can be viewed in the online issue, which is available at wileyonlinelibrary.com.]

that is, with Variant 1 of the proposed technique. This route requires only the plant output data and no other information about the system. It also requires less data with a coarser sampling than the other routes, as indicated earlier. In that sense, it is the most desirable technique to be applied on the data.

Systems 1 and 2 are multivariate systems with two outputs (y_1 and y_2). However, it can be observed[26] that for both the systems the output y_1 shows a significant dependence on the parameter K_{12}, while y_2 is relatively insensitive to controller tuning. So, only $\epsilon_1(t)=y_1^{\text{ref}}(t)-y_1(t)$ is considered for identifying the optimal conditions of the controller for both Systems 1 and 2.

Figure 5 shows the results of data segmentation and identification from the plant output error data for System 1. There are 11 different configurations of the system. It can be seen from the plots that with deterioration of controller performance, there is an increase in variance of the signal. This time dependence of variance is exploited to identify segments of stationary data in the signal. It can be observed that the technique is able to segment the data, as well as identify the optimum window very efficiently. There is a loss of the ability to identify segments properly for three cases when the variance is relatively insensitive to the tuning. However, as the location of optimal window is changed to a region where there is a better sensitivity of variance to tuning, the segmentation and identification is achieved properly.

It is important to note here that with the above results one cannot quantify the controller performance in the windows—the MVI or scaling exponent have to be evaluated in every window to assess the performance. As MVI needs the knowledge of system delay, this makes it a less attractive option when implemented over numerous loops.

The plots for System 2 are shown in Figure 6. The variance of data can be observed to be relatively insensitive for three cases, like System 1 and hence the identification is not proper for the first three cases. In addition to this, the data for the true

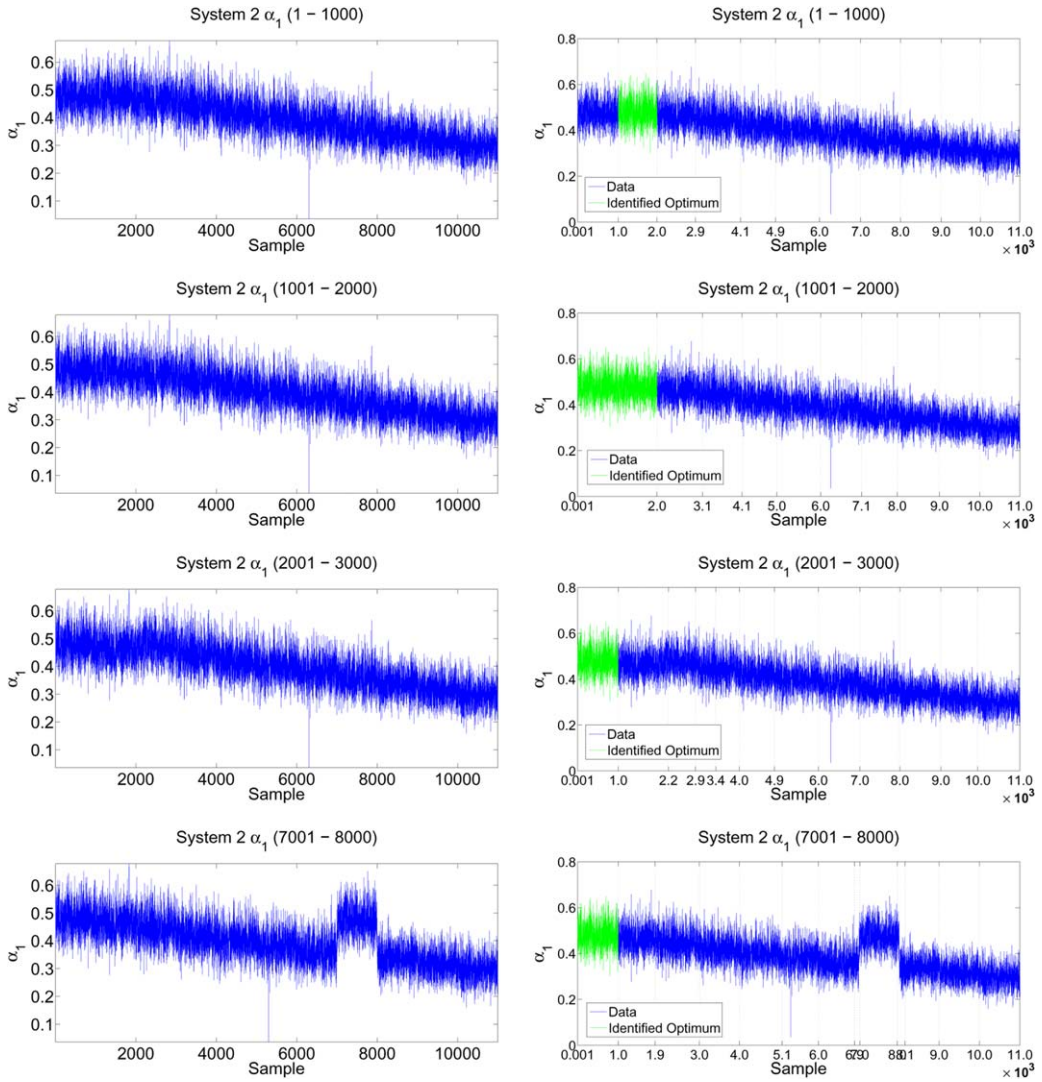

Figure 9. Identification of data segment corresponding to optimal configuration for System 2 using scaling exponent data ($\alpha_1(t)$).

Left column plots show the raw data and right column plots show the data after segmentation and identification. Green portion represents the identified optimal settings while the true optimal settings for each case are specified in the title of each plot. For example, in the last plot, true optimum lies in 7001–8000 and identified optimum is 1–1000. However, the true optimum window is identified as a separate segment. [Color figure can be viewed in the online issue, which is available at wileyonlinelibrary.com.]

optimum is not the one with the minimum variance in certain cases. This might be an artifact of finite sample effects. Notice, however, that the interval halving technique does identify the optimal window as a separate segment of stationary data, as expected.

Sample output error for Systems 3 (seven configurations) and 4 (six configurations) are shown in Figure 7. With poor tuning of the controller, the variance of the error output is expected to increase. However, the amount by which the variance increases is very less in these cases, and is not significant enough to be detectable by the interval halving algorithm for the proposed technique to work. The proposed variant based on variance of the signal therefore cannot be reliably applied to Systems 3 and 4.

Simulation results: Variant 2 (scaling exponent or MVI)

The plant output error exhibited variance nonstationarity, while the scaling exponent and MVI indices both display mean nonstationarity in the presence of multiple configurations. We demonstrate the proposed technique on scaling exponent data for all the systems and the MVI data on the univariate systems (Systems 3 and 4).

All the systems are simulated for 1000 data points, and the scaling exponent and MVI (MVI for SISO systems—Systems 3 and 4 only) of the plant output are calculated. This procedure is repeated for 1000 times with the same controller configuration to obtain a time series of scaling exponents, with a constant mean and finite variance. This is equivalent to having a larger number of contiguous ϵ data points. The tuning is then changed and the above exercise is repeated.

Only α_1 is considered for identifying the optimal conditions of the controller for both Systems 1 and 2. Eleven controller settings have been considered resulting in a 11,000 $\times$ 1 time series. The arrangement of these 11 settings is varied to mimic different evolutions of controller parameters. This signal is then processed for identifying the optimal window.

The results of identification of the optimal conditions for Systems 1 and 2 with the scaling exponent route are shown

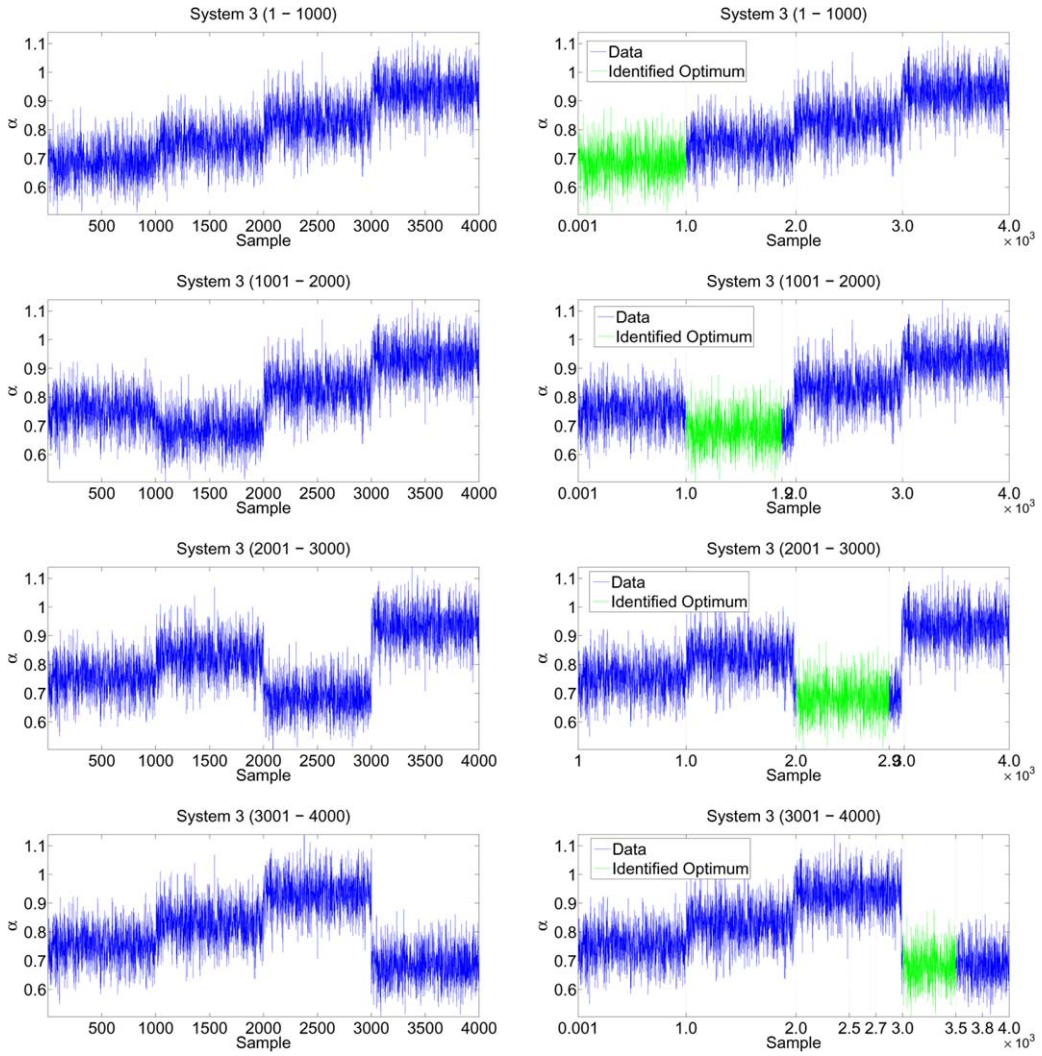

Figure 10. Identification of data segment corresponding to optimal configuration for System 3 using scaling exponent data ($\alpha(t)$).

Left column plots show the raw data and right column plots show the data after segmentation and identification. Green portion represents the identified optimal settings while the true optimal settings for each case are specified in the title of each plot. For example, in the last plot, true optimum lies in 3001–4000 and identified optimum is 3001–3500. [Color figure can be viewed in the online issue, which is available at wileyonlinelibrary.com.]

in Figures 8 and 9, respectively. From Figure 8, it is clear that in the first two cases, the data are relatively insensitive to tuning, that is, almost same for both the configurations. Moreover, as these data are located adjacent to each other in time, the technique is not able to distinguish between the two segments. However, when the two segments are located distant in time, the technique is able to correctly identify the optimal region. Note that the distinct regions where the data is stationary are also identified correctly. So, the scaling exponent route works very efficiently for System 1.

For System 2, the data are relatively insensitive for two cases and like System 1, the identification is not proper for the first two cases. This effect was also observed with the output error data for System 2. However, for all the cases shown in Figure 9, the identified window is different from the true optimal window. This is because of the fact that in the data for the true optimum the average scaling exponent is not the closest to the optimum value of 0.5. This effect is not expected, but observed with this system. Notice, however, that the interval halving technique does identify the optimal window as a separate segment of stationary data, as expected.

System 3 is simulated with five controller configurations and the arrangement of these settings is varied to mimic different evolutions of the controller configuration. The results obtained for System 1 are shown in Figure 10. From Figure 10, it is clear that the interval halving procedure identifies the segments of stationary data very efficiently. The same can be said about plots for System 4 in Figure 11.

Figures 12 and 13 show the results of the tool applied on MVI data for Systems 3 and 4, respectively, which also indicate excellent performance of the technique. For example, in the first case in Figure 12, the controller performance is continuously deteriorating, and the MVI is moving away from 1. The proposed technique is able to identify the segments with relatively constant MVI and also the segment that is closest to the theoretical optimum of 1. In all the scenarios, the technique is able to segment the data very efficiently and also identify the optimal segment. However, it must be noted that in evaluating the MVI, knowledge of

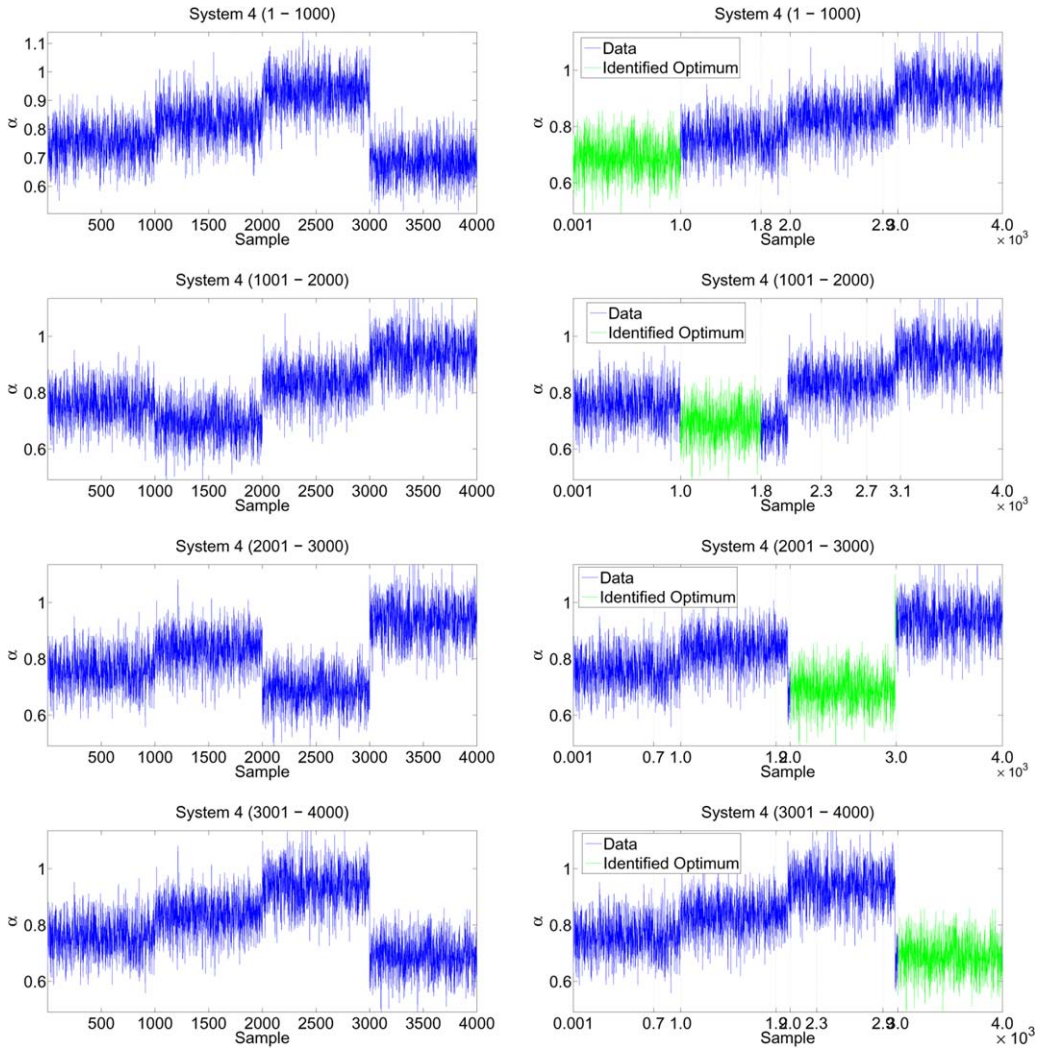

Figure 11. Identification of data segment corresponding to optimal configuration for System 4 using scaling exponent data ($\alpha(t)$).

Left column plots show the raw data and right column plots show the data after segmentation and identification. Green portion represents the identified optimal settings while the true optimal settings for each case are specified in the title of each plot. For example, in the last plot, true optimum lies in 3001–4000 and identified optimum is 3001–4000. [Color figure can be viewed in the online issue, which is available at wileyonlinelibrary.com.]

system delay is necessary, which is not the case with scaling exponent route.

Remark 3. *All the simulation studies presented in this work have a parametric variation as the cause of nonstationarity. However, even if the nonstationarity is due to sources other than changes in plant-controller settings (such as disturbances) the proposed techniques will be able to identify the segments of stationary regions and a performance assessment in each region can be performed using scaling exponent/MVI. This is because the proposed technique relies solely on the output data or the performance indices for data segmentation and does not discriminate nonstationarity based on its source.*

Remark 4. *When the scaling exponent is used to assess the performance of a control loop, there is a small but finite mismatch between the MVI and* α[19] *when the loop is operating very close to the true optimum. This is illustrated in the following sections for System 4 where the identified optimum is 3007–3991 while the true optimum is 1–1000. If the system delay is known, then the MVI route will offer a better result than* α *route. However, if the tool has to be employed on large-scale data for thousands of loops, using the scaling exponent route and noting that there can be a small mismatch would be more appealing than providing the delay for all the loops and calculating the MVI's.*

Experimental Validation

The proposed technique has been tested on a temperature control experiment in a laboratory at Indian Institute of Technology Gandhinagar. The control objective is to maintain the temperature of a liquid (in this case water) inside a chamber at a desired set point. The experimental setup includes a resistance-based temperature sensor that detects the temperature and generates an equivalent electric signal. A desktop PC is used to process the data using LabVIEW® and appropriate control moves are decided based on Proportional integral derivative (PID) controller scheme. The data from sensor (collected at a rate of 20 samples per second) and the control

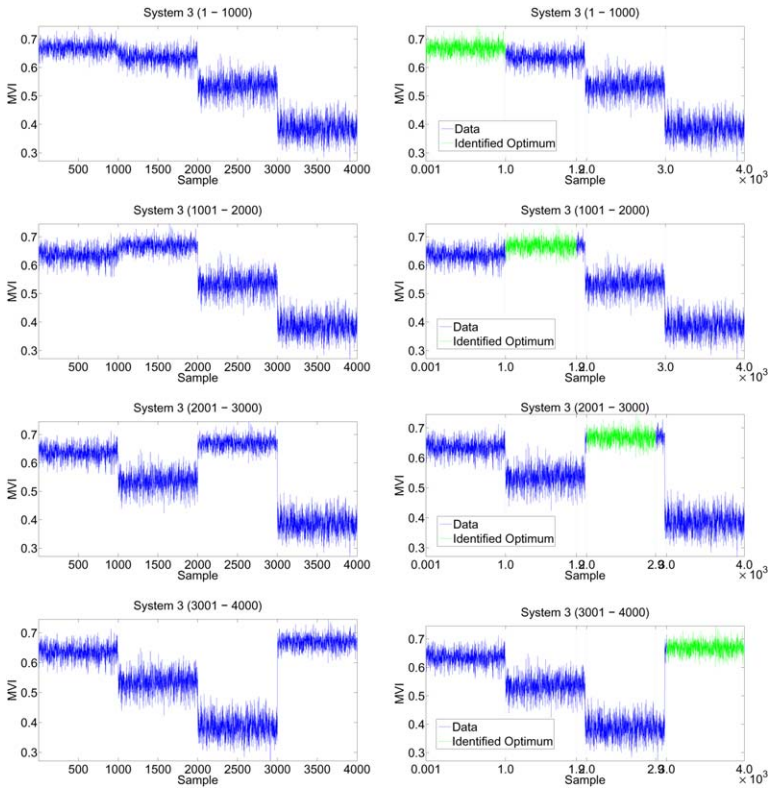

Figure 12. Identification of data segment corresponding to optimal configuration for System 3 using MVI data (MVI(t)).

Left column plots show the raw data and right column plots show the data after segmentation and identification. Green portion represents the identified optimal settings while the true optimal settings for each case are specified in the title of each plot. For example, in the last plot, true optimum lies in 3001–4000 and identified optimum is 3001–4000. [Color figure can be viewed in the online issue, which is available at wileyonlinelibrary.com.]

moves are communicated through a NI® Data Acquisition (DAQ) device. A heater and a fan are used as actuators to achieve the desired temperature control.

A set point of 60°C is used and the PID controller is tuned such that the temperature is maintained at the set point. The controller settings are then changed and data are acquired with DAQ for every configuration. Three such configurations have been used in the experiment. The scaling exponent has been calculated for the output data in each case and they are concatenated and shown in Figure 14. In estimating the scaling exponent using DFA, a moving window of 1000 samples has been used that is shifted every 10 samples and 500 samples of scaling exponent are obtained as described in Remark 1. The proposed technique is applied on the Hurst exponent data and results obtained are plotted in Figure 14.

From Figure 14, it is clear that the scaling exponent exhibits mean nonstationarity, as expected. The proposed technique is able to identify the different segments effectively. Although there are more windows identified than necessary, this can be attributed to presence of environmental disturbances in the experiment. However, the identified portion coincides with the true optimum segment.

Discussion

In this section, we list a few observations along with certain criteria that have to be satisfied by the data for each variant to yield proper results. Finally, the effect of certain tuning parameters on the results obtained is presented.

Observations

The proposed technique uses three routes—the scaling exponent (α), MVI, and output error variance (σ_ϵ^2)—to characterize the controller performance and a significant deviation in these parameters to detect a change in configuration. A comparison of these routes and a few inferences drawn are outlined below.

- The parameter of interest may or may not be sensitive to the controller tuning. If a parameter is not sensitive to the tuning, then the corresponding variant cannot be employed to identify the optimum window. This is because the data does not contain enough *information* about the controller configuration. However, the alternate routes can be adopted to achieve the goal. This effect was observed for Systems 3 and 4 when the raw plant output data was used.
- If the parameter is sensitive to the tuning, then all variants can be employed. Here, two cases arise:
  - *the optimal parameters correspond to the true optimal tuning*: In this case, the scaling exponent route performs slightly better than the plant output route (System 1). However, assuming that 1000 data points are needed to compute a single scaling exponent, appropriate number of samples (can be achieved using a moving window) are required for utilization of this approach.
  - *Identified optimal region does not correspond to the true optimal region*: theoretically, this is not expected as the measures used (scaling exponent and variance of the error signal) are representative of the performance of the control loop. However, when the controller is operating very close

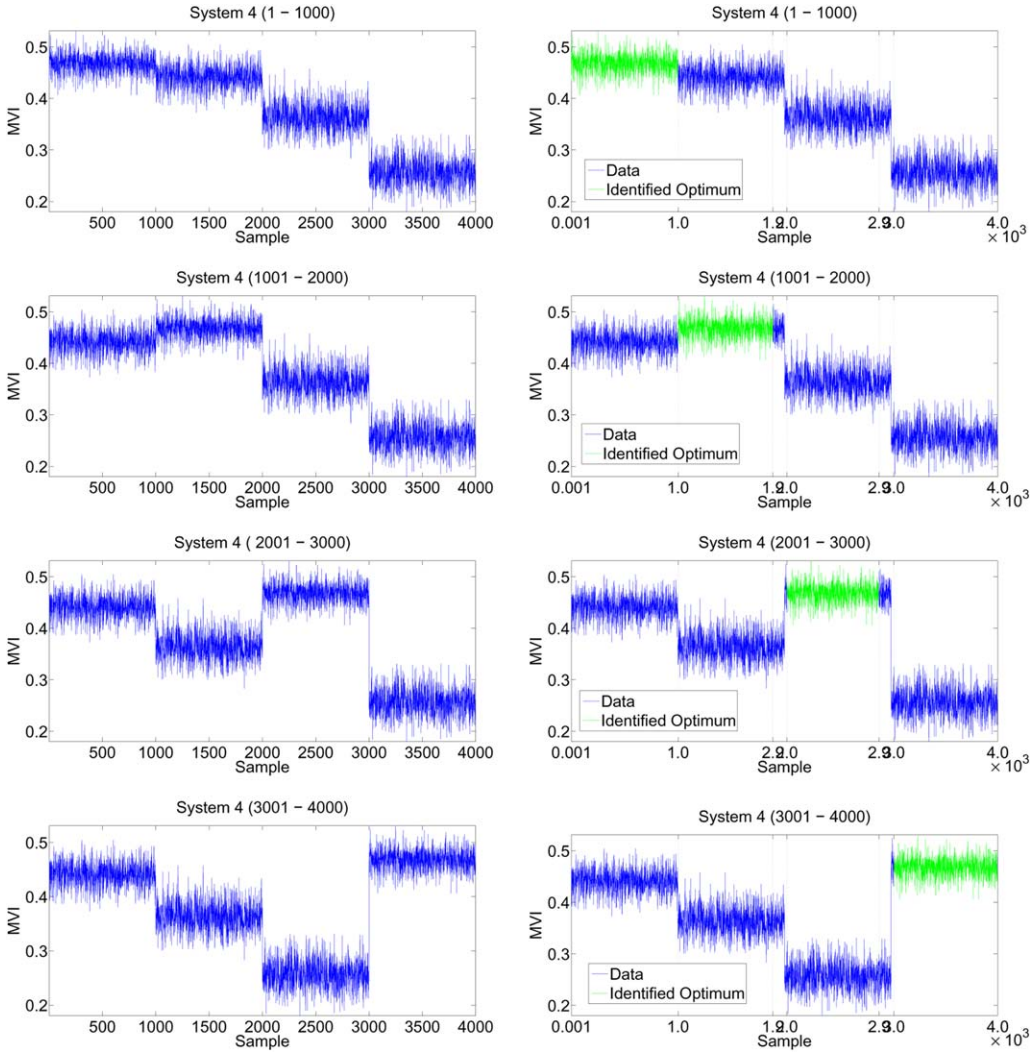

Figure 13. Identification of data segment corresponding to optimal configuration for System 4 using MVI data (MVI(*t*)).

Left column plots show the raw data and right column plots show the data after segmentation and identification. Green portion represents the identified optimal settings while the true optimal settings for each case are specified in the title of each plot. For example, in the third plot, true optimum lies in 2001–3000 and identified optimum is 2001–2900. [Color figure can be viewed in the online issue, which is available at wileyonlinelibrary.com.]

to the true optimum then due to finite sample effects there can be ambiguity in deciding the optimum window. Also as presented in Ref. 19, there is a minor mismatch between the MVI and scaling exponent[19] which occurs due to the latter being a delay free measure of performance, which can obscure the identification procedure, though the identified optimal dataset will be close to the true optimal region. (These cases have not been included in the results, but demonstrated in the following sections.)

The MVI route as well as the scaling exponent route involve evaluating a performance index and then performing interval halving. However, when the tool is to be employed on thousands of loops, the latter option is the obvious choice as this does not need the knowledge of system delay for each of the loops.

- Although segmentation of data can be performed with both the methods, quantifying the scope of improvement in performance without knowledge of the system delay is not possible by just analyzing the variance of the error signal. In that respect, the scaling exponent route offers a complete solution to the questions pertaining to CLPA indicated earlier, assuming minimum possible information about the system.

Choice of window size

The interval halving algorithm terminates when a prespecified minimum window size is reached (to ensure termination of the algorithm). As a result, if the data within a window of this size is nonstationary, it will not be detected by the technique. This places a lower bound on the detectable rate at which the plant changes. If the plant changes at a rate such that data chunks of size smaller than the minimum allowable size are nonstationary, then the technique will not be able to detect the presence of nonstationarity. The selection of the window size, therefore, plays an important role in deploying the technique—very small window sizes will provide better resolution at an elevated computational cost while too large window sizes will lead to loss of resolution. The latter being a more severe problem, it is advisable to have minimum window sizes that can be

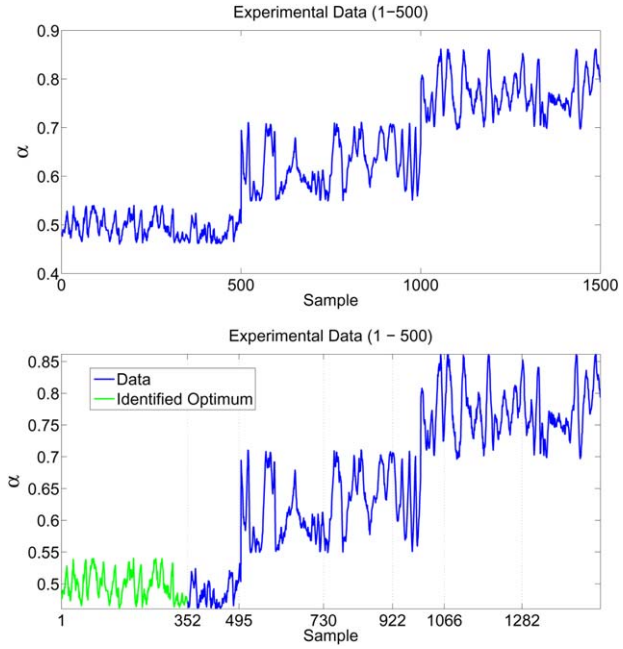

Figure 14. Identification of data segment corresponding to optimal configuration for experimental data using Scaling exponent data ($\alpha(t)$).

Top plot shows the raw data and bottom plot shows the data after segmentation and identification. Green portion represents the identified optimal settings while the true optimal setting is from 1 to 500 as indicated in the title of each plot. [Color figure can be viewed in the online issue, which is available at wileyonlinelibrary.com.]

accommodated by the computational device and possibly knowledge of the approximate rate of change of plant behavior. However, in this work, we do not choose any prespecified optimal window size for segmentation and the optimal data segments are automatically identified by the algorithm.

Effect of tuning parameters

The major tuning parameters in the proposed technique are: (1) minimum window size in interval halving approach and (2) significance level in statistical tests (Goodness of Fit and *t* test). The minimum window size during interval halving can be set to a very small value, such as 10 or 20 so as to allow small windows to be identified. However, this increases the

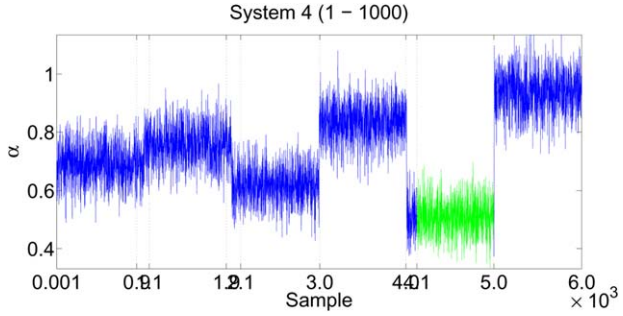

Figure 15. Ambiguity with scaling exponent when operating too close to optimality (for System 4).

[Color figure can be viewed in the online issue, which is available at wileyonlinelibrary.com.]

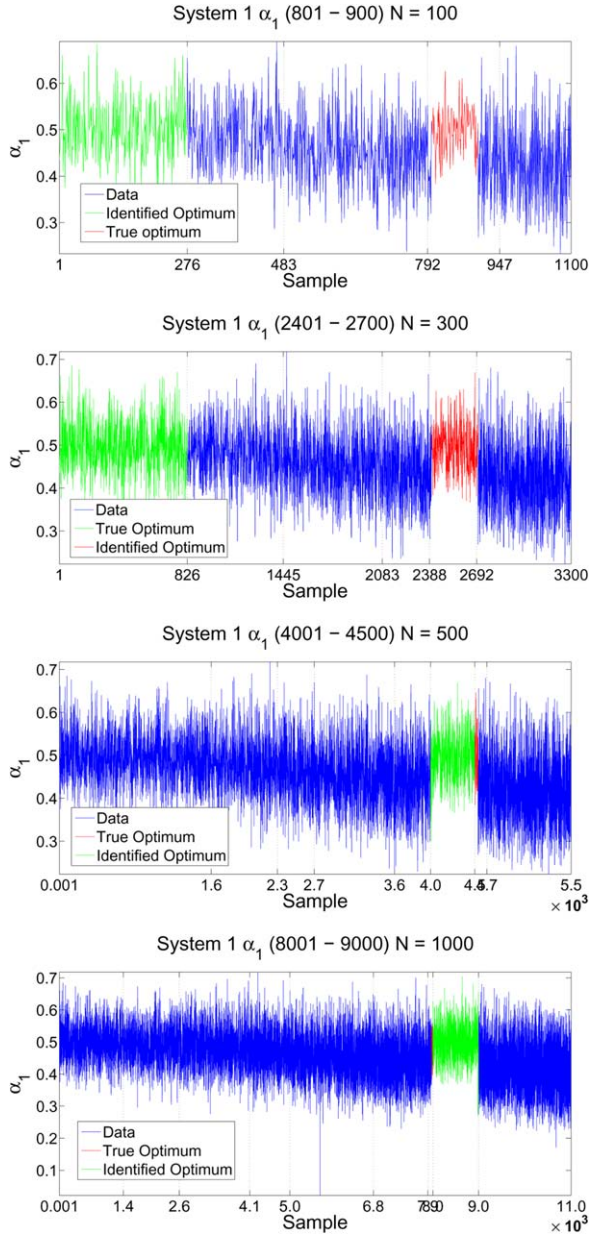

Figure 16. Effect of number of data points available on the efficiency of the proposed method for the scaling exponent data for System 1, α_1. [Color figure can be viewed in the online issue, which is available at wileyonlinelibrary.com.]

computational burden and hence there is a trade-off between the available computational power and the required resolution. In this work, a minimum window size of 100 samples is used. For all the statistical tests, a significance level of 95% is used.

Both the tuning parameters depend on the amount of data available and, therefore, the number of samples pertaining to the optimal configuration plays a major factor affecting the efficiency of the proposed method. The effect of the optimal data size on the results from scaling exponents is illustrated in Figure 16 while its influence on the variance of the error analysis is presented in Figure 17. The number of data points is varied and the identification procedure is performed for the same evolution of controller configuration for 100, 300, 500,

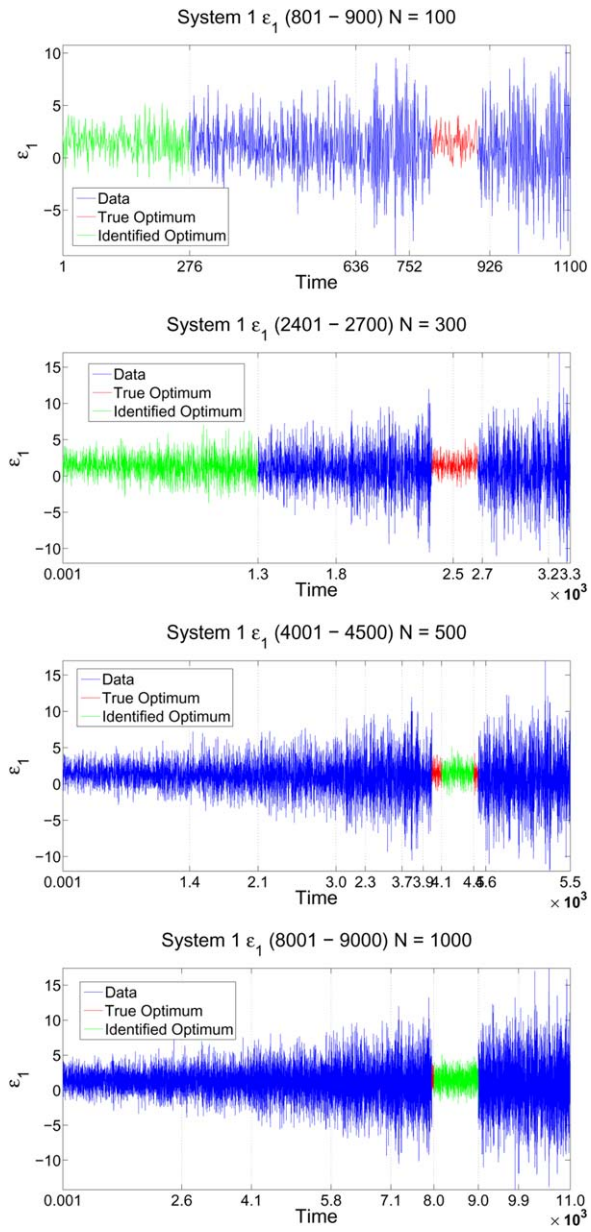

Figure 17. Effect of number of data points available on the efficiency of the proposed method for the plant output data for System 1, ϵ_1.

The red portion is true optimum and green portion is identified optimum. The number of data points considered for each case is mentioned in the title of each plot. As the number of data points for each configuration increases, the identified optimum converges to true optimum window. [Color figure can be viewed in the online issue, which is available at wileyonlinelibrary.com.]

and 1000 points. In the figures, the portion indicated in red is the true optimum while that in green is the one identified as optimum by the proposed method. As can be observed from Figures 16 and 17, the number of data points available for optimal configuration (N) affects the region of the data identified as the optimal window. Initially, the identification is incorrect, while as the number of data points increase, the segment identified by the proposed technique as the optimum segment converges on the true optimum. From both the cases, the minimum number of samples required can be inferred as 500. From this analysis, it is clear that there should be sufficient number of samples corresponding to optimal controller settings for its identification without any ambiguities.

Framework for application

We describe a framework in which the proposed technique can be applied to perform data segmentation and identification of optimal window. The route involving ϵ is the first choice as it requires least amount of data as well as information about the system. If the variance of ϵ is not sensitive enough, the scaling exponent route is the next choice as it does not need the system delay to be known. However, if one is willing to provide the system delay for numerous control loops in a large scale scenario, then the MVI route can be adopted.

The proposed variance route allows data segmentation before any CLPA is performed and can be used as a preprocessing technique for CLPA. On the contrary, the latter two routes involve evaluating the performance indices and then performing data mining. This is helpful for identification of optimal configurations for the purpose of user-defined benchmarking. However, using the ϵ data and calculating the indices based on a moving window, one might also be able to use these techniques as a data preprocessing tool. Flowchart 4 shows a framework for applying the proposed technique to control loop data.

It should be noted that every route has its own drawbacks—the using variance route (ϵ) provides less information and could be insensitive to certain systems, the scaling exponent (α) route needs comparitively large amounts of data and the MVI route requires knowledge of system delay, obtaining which can be prohibitively complicated for large systems. As a result, our conclusion is that the method of choice should be based on the characteristics of the application that is being solved. Nonetheless, we believe that we have provided a robust set of tools that can be used, collectively, to address a large cross-section of industrial problems of interest.

The proposed framework could also be modified to become an online approach. An example of such a modification to interval halving algorithm is already available.[33] However, in this article, we perform just an offline analysis. The offline analysis by itself is very useful and can be used to derive a variety of diagnostic measures. For example, a metric can be derived to identify loops that have performed consistently well for a large amount of time. The reasons for the success of such loops can be analyzed and, if possible, translated to other loops. Similarly, loops that perform consistently poorly can be identified and diagnosis can be performed to see if this is a result of poor operational strategies or if there are some fundamental design limitations that have to be addressed. The analysis that is performed using the techniques proposed in this article can then be used to derive economic metrics that will aid in answering questions such as is it worthwhile to make design modifications to improve the performance of some loops. These types of analysis are over and above fundamental benchmarking (the best that a loop has ever performed given the current plant configuration) that can be performed using these techniques. These benchmarks can then be used to drive individual loops toward their ideal behavior. Further, in an industrial setting with advanced controllers (such as Model Predictive Controllers), application of this framework on base level PI/PID controllers could help distinguish performance issues due to base level (PI/PID) and advanced controller with constraints.

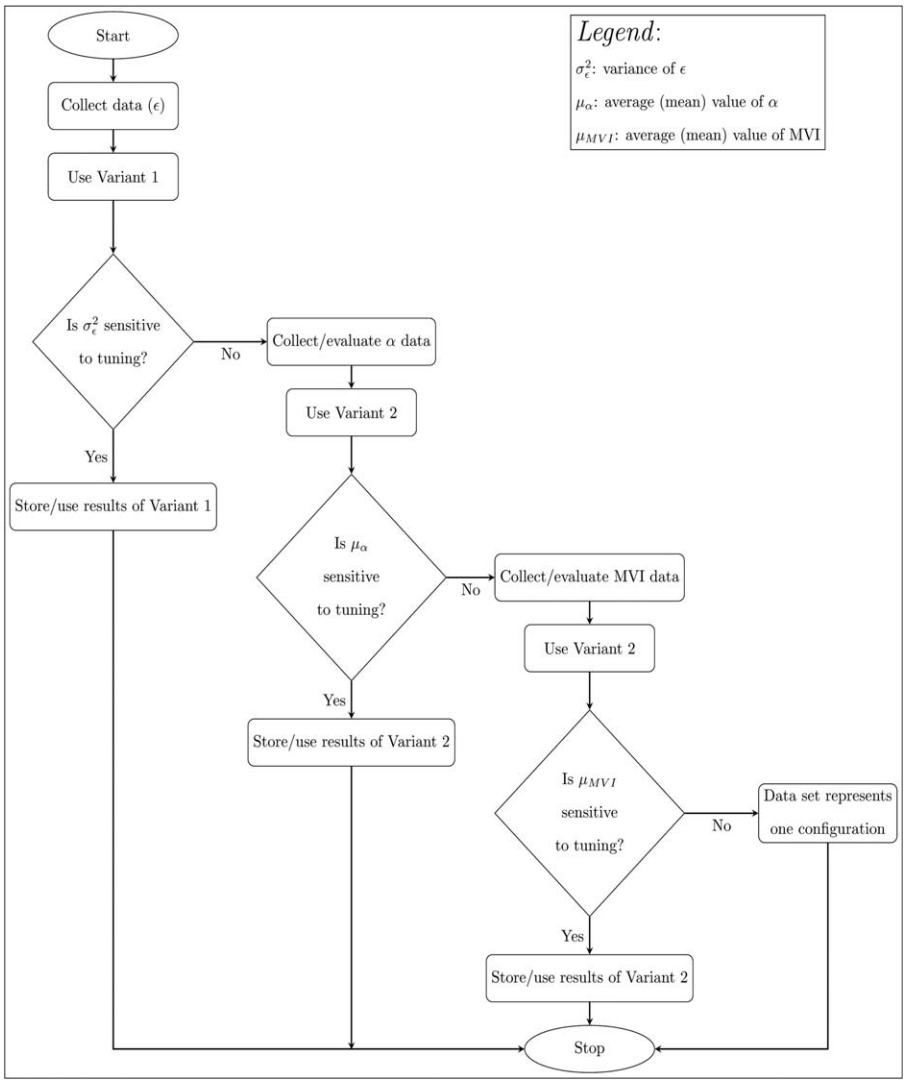

Flowchart 17. Framework for applying the proposed technique.

Conclusions

The fundamental issue of data selection for CLPA was addressed. A technique for segmenting the nonstationary plant output data into stationary windows and further identifying the segment representative of optimal controller settings was developed. The technique uses interval halving to identify windows in time over which the signal of interest is stationary, and then finds those regions corresponding to the optimal tuning condition. This is performed using analysis of: (1) variance of the error signal (ϵ), (2) scaling exponent of the error, and (3) MVI computed from the error. The output error route requires least data and not knowledge about the system and is therefore the most desirable approach. However, if the variance is not sensitive enough to tuning, the results can be misleading. Moreover, the controller performance cannot be assessed in every window identified with the technique. The scaling exponent data allows simultaneous assessment of the performance of the controller with the theoretical benchmark without any other information about the plant and in that sense is much superior to the MVI route. Conversely, the MVI route always identifies the region corresponding to optimal controller settings, but requires the system delay to be known, which might not be possible for a system with a large number of loops.

The proposed technique, however, does not propose a method to account for interactions between control loops in a multivariate system. Moreover, inclusion of constraints for applying the technique to advanced process control methods is not addressed in this work, which remain as future work.

The red portion is true optimum and green portion is identified optimum. The number of data points considered for each case is mentioned in the title of each plot. As the number of data points for each configuration increases, the identified optimum converges to true optimum window. [Color figure can be viewed in the online issue, which is available at wileyonlinelibrary.com.]

Acknowledgment

The authors would like to extend their gratitude to Mr. S. Rajendran and Mr. Pragnesh Parekh for their support and assistance in the experimental work at the Electrical Engineering Laboratory, Indian Institute of Technology, Gandhinagar, India.

Literature Cited

1. Desborough L, Miller R. Increasing customer value of industrial control performance monitoring—Honeywells experience. *AIChE Symposium Series No. 326*, New York, USA: American Institute of Chemical Engineers, *Vol. 98*. 2001:169–189.
2. Harris T, Seppala C, Desborough L. A review of performance monitoring and assessment techniques for univariate and multivariate control systems. *J Process Control*. 1999;9(1):1–17.
3. Harris T. Assessment of closed loop performance. *Can J Chem Eng*. 1989;67:856–861.
4. Jain M, Lakshminarayanan S. A filter-based approach for performance assessment and enhancement of SISO control systems. *Ind Eng Chem Res*. 2005;44(22):8260–8276.
5. Ko BS, Edgar T. PID control performance assessment: the single-loop case. *AIChE J*. 2004;50:1211–1218.
6. Harris T, Boudreau F, MacGregor J. Performance assessment of multivariable feedback controllers. *Automatica*. 1996;32(11):1505–1518.
7. Huang B, Shah SL, Kwok EK. On-line control performance monitoring of MIMO processes. In: *Proceedings of the American Control Conference, 1995*, *Vol. 2*. Seattle, Washington, USA: IEEE, 1995:1250–1254.
8. Thornhill N, Oettinger M, Fedenczuk P. Refinery-wide control loop performance assessment. *J Process Control*. 1999;9(2):109–124.
9. Huang B, Shah S, Kwok E. Good, bad or optimal? Performance assessment of multivariable processes. *Automatica*. 1997;33(6):1175–1183.
10. Huang B, Ding SX, Thornhill N. Alternative solutions to multivariate control performance assessment problems. *J Process Control*. 2006;16(5):457–471.
11. Harris T, Yu W. Controller assessment for a class of nonlinear systems. *J Process Control*. 2007;17:607–619.
12. Wood R, Berry M. Terminal composition control of a binary distillation column. *Chem Eng Sci*. 1973;28(9):1707–1717.
13. DeVries W, Wu S. Evaluation of process control effectiveness and diagnosis of variation in paper basis weight via multivariate time-series analysis. *IEEE Trans Autom Control*. 1978;23(4):702–708.
14. Huang B, Shah SL, Kwok KE, Zurcher J. Performance assessment of multivariate control loops on a paper-machine headbox. *Can J Chem Eng*. 1997;75(1):134–142.
15. Jelali M. Performance assessment of control systems in rolling mills–application to strip thickness and flatness control. *J Process Control*. 2007;17(10):805–816.
16. Joe Qin S. Control performance monitoring—a review and assessment. *Comput Chem Eng*. 1998;23(2):173–186.
17. Jelali M. An overview of control performance assessment technology and industrial applications. *Control Eng Pract*. 2006;14:441–466.
18. Jain M, Lakshminarayanan S. Estimating performance enhancement with alternate control strategies for multiloop control systems. *Chem Eng Sci*. 2007;62(17):4644–4658.
19. Srinivasan B, Spinner T, Rengaswamy R. Control loop performance assessment using detrended fluctuation analysis (DFA). *Automatica*. 2012;48(7):1359–1363.
20. Pillay N, Govender P. A data driven approach to performance assessment of PID controllers for setpoint tracking. *Procedia Eng*. 2014;69:1130–1137.
21. Hurst HE. Methods of using long-term storage in reservoirs. In: *ICE Proceedings, Vol. 5*. Thomas Telford, 1956:519–543.
22. Abry P, Veitch D. Wavelet analysis of long-range-dependent traffic. *IEEE Trans Inf Theory*. 1998;44(1):2–15.
23. Abry P, Flandrin P, Taqqu MS, Veitch D. Self-similarity and long-range dependence through the wavelet lens. In: Doukhan P, Openheim G, Taqqu MS, editors. *Theory and Applications of Long-Range Dependence*. Boston: Birkhaüser, 2003:527–556.
24. Peng C, Buldyrev S, Goldberger A, Havlin S, Sciortino F, Simons M, Stanley H. Long-range correlations in nucleotide sequences. *Nature*. 1992;356(6365):168–170.
25. Sendjaja AY, Kariwala V. Achievable PID performance using sums of squares programming. *J Process Control*. 2009;19(6):1061–1065.
26. Huang B, Shah SL. *Performance Assessment of Control Loops: Theory and Applications*. London: Springer, 1999.
27. Keogh E, Chu S, Hart D, Pazzani M. An online algorithm for segmenting time series. In: *Proceedings IEEE International Conference on Data Mining 2001, ICDM 2001*. San Jose, California, USA: IEEE, 2001:289–296.
28. Andrews DW. Tests for parameter instability and structural change with unknown change point. *Econometrica*. 1993;61:821–856.
29. Allahyari S, Amiri A. A clustering approach for change point estimation in multivariate normal processes. In: *Proceedings of the 41st International Conference on Computers & Industrial Engineering*, Los Angeles, California, USA, 2014.
30. Preuß P, Puchstein R, Dette H. Detection of multiple structural breaks in multivariate time series. *J Am Stat Assoc*. 2014;110.
31. Dash S, Maurya MR, Venkatasubramanian V, Rengaswamy R. A novel interval-halving framework for automated identification of process trends. *AIChE J*. 2004;50(1):149–162.
32. Villez K, Venkatasubramanian V, Rengaswamy R. Generalized shape constrained spline fitting for qualitative analysis of trends. *Comput Chem Eng*. 2013;58:116–134.
33. Maurya MR, Paritosh PK, Rengaswamy R, Venkatasubramanian V. A framework for on-line trend extraction and fault diagnosis. *Eng Appl Artif Intell*. 2010;23(6):950–960.
34. Gamero FI, Meléndez J, Colomer J. Process diagnosis based on qualitative trend similarities using a sequence matching algorithm. *J Process Control*. 2014;24(9):1412–1424.
35. Godfrey LG, Orme CD. The robustness, reliabiligy and power of heteroskedasticity tests. *Econom Rev*. 1999;18(2):169–194.
36. Breusch TS, Pagan AR. A simple test for heteroscedasticity and random coefficient variation. *Econometrica*. 1979;47:1287–1294.

Manuscript received Apr. 30, 2015, and revision received July 27, 2015.